BIOCHEMISTRY
including biophysical chemistry & molecular biology

Article

pubs.acs.org/biochemistry

Covalent Conjugation of a Peptide Triazole to HIV-1 gp120 Enables Intramolecular Binding Site Occupancy

Ali Emileh,*[,†,‡,∥] Caitlin Duffy,[‡] Andrew P. Holmes,[‡] Arangassery Rosemary Bastian,[‡,§] Rachna Aneja,[‡] Ferit Tuzer,[‡] Srivats Rajagopal,[‡] Huiyuan Li,[‡] Cameron F. Abrams,*[,†,‡] and Irwin M. Chaiken*[,‡]

[†]Chemical and Biological Engineering, Drexel University, Philadelphia, Pennsylvania 19104, United States

[‡]Biochemistry and Molecular Biology, Drexel University College of Medicine, Philadelphia, Pennsylvania 19129, United States

[§]School of Biomedical Engineering, Science and Health Systems, Drexel University, 3141 Chestnut Street, Philadelphia, Pennsylvania 19104, United States

Supporting Information

ABSTRACT: The HIV-1 gp120 glycoprotein is the main viral surface protein responsible for initiation of the entry process and, as such, can be targeted for the development of entry inhibitors. We previously identified a class of broadly active peptide triazole (PT) dual antagonists that inhibit gp120 interactions at both its target receptor and coreceptor binding sites, induce shedding of gp120 from virus particles prior to host−cell encounter, and consequently can prevent viral entry and infection. However, our understanding of the conformational alterations in gp120 by which PT elicits its dual receptor antagonism and virus inactivation functions is limited. Here, we used a recently developed computational model of the PT−gp120 complex as a blueprint to design a covalently conjugated PT−gp120 recombinant protein. Initially, a single-cysteine gp120 mutant, E275C$_{YU-2}$, was expressed and characterized. This variant retains excellent binding affinity for peptide triazoles, for sCD4 and other CD4 binding site (CD4bs) ligands, and for a CD4-induced (CD4i) ligand that binds the coreceptor recognition site. In parallel, we synthesized a PEGylated and biotinylated peptide triazole variant that retained gp120 binding activity. An N-terminally maleimido variant of this PEGylated PT, denoted AE21, was conjugated to E275C gp120 to produce the AE21−E275C covalent conjugate. Surface plasmon resonance interaction analysis revealed that the PT−gp120 conjugate exhibited suppressed binding of sCD4 and 17b to gp120, signatures of a PT-bound state of envelope protein. Similar to the noncovalent PT−gp120 complex, the covalent conjugate was able to bind the conformationally dependent mAb 2G12. The results argue that the PT−gp120 conjugate is structurally organized, with an intramolecular interaction between the PT and gp120 domains, and that this structured state embodies a conformationally entrapped gp120 with an altered bridging sheet but intact 2G12 epitope. The similarities of the PT−gp120 conjugate to the noncovalent PT−gp120 complex support the orientation of binding of PT to gp120 predicted in the molecular dynamics simulation model of the PT−gp120 noncovalent complex. The conformationally stabilized covalent conjugate can be used to expand the structural definition of the PT-induced "off" state of gp120, for example, by high-resolution structural analysis. Such structures could provide a guide for improving the subsequent structure-based design of inhibitors with the peptide triazole mode of action.

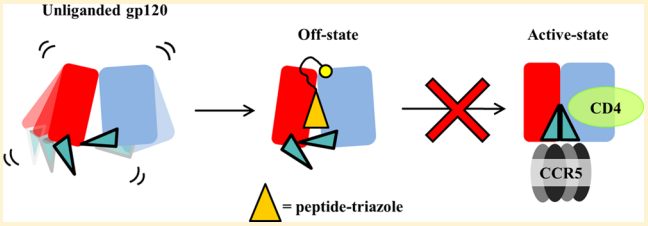

HIV entry is mediated by envelope spikes on the surface of the virus.[1,2] Each spike is a noncovalent trimer of gp120 and gp41 dimers.[1] Binding of gp120 to CD4 on target cells triggers a sequence of conformational changes in the spike that lead to binding of gp120 to the coreceptor (a member of the chemokine receptor family, usually CCR5 or CXCR4), and consequent fusion of the viral and cell membranes, leading to cell infection.[3] This multistep process provides a series of targets for blocking infection before the virus establishes a foothold in the host.[4]

Dual antagonist peptide triazoles (PTs) make up a novel class of broadly active and nontoxic[5,6] gp120 binding entry inhibitors that simultaneously inhibit interactions of gp120 at the binding sites for both CD4 and the coreceptor (CCR5 or CXCR4).[7,8] These compounds exhibit submicromolar antiviral activities against HIV-1 clades A−D, including transmitted/founder viruses. Members of this family bind to soluble gp120$_{YU-2}$ with low nanomolar affinity and can be synergistically combined with other entry inhibitors.[5,6] At the virus level, the PTs cause gp120 shedding, and some variants exhibit virolytic activity.[9] Peptide triazoles have been found to bind to a highly conserved site that overlaps the CD4 binding site on gp120.[10] All these properties make PTs attractive leads for both therapeutic and microbicidal applications.

Received: January 31, 2014
Revised: April 27, 2014
Published: May 6, 2014

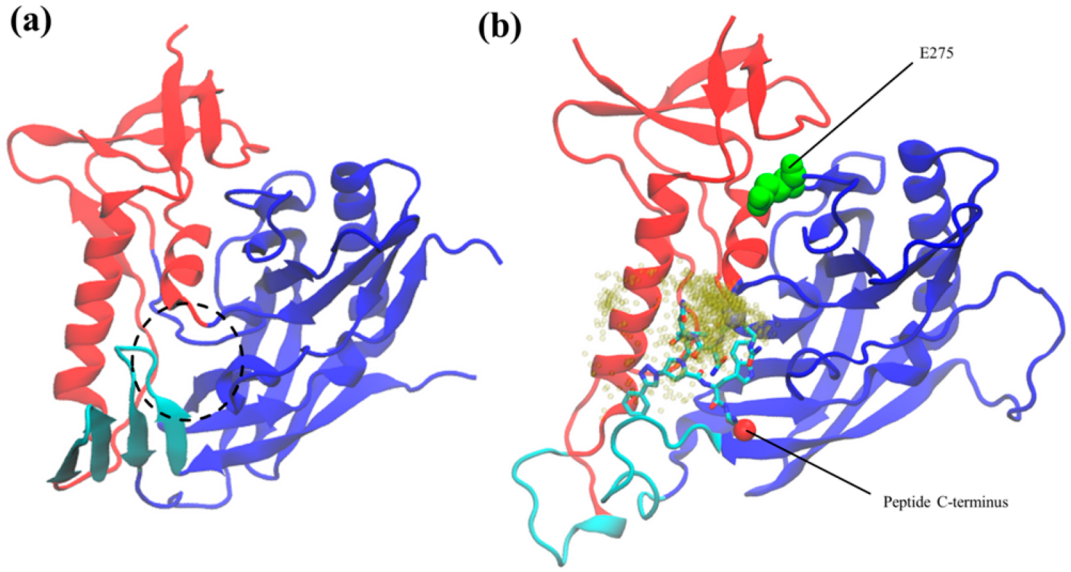

Figure 1. (a) gp120 core in the CD4-bound activated state. The approximate location of the F43 pocket is shown with the dashed black circle. (b) Modeled lowest-energy conformation of the peptide triazole–$gp120_{YU-2}$ core encounter complex from ref 16. The small yellow spheres show the locus of the N-terminal nitrogen atom of the peptide backbone during the 200 ns MD equilibration performed in this study. The peptide sequence used in simulations is that of UM101 (Table 1). Residue E275 is shown as green spheres. The peptide triazole is depicted as sticks, with the N- and C-terminal amine nitrogen and carbonyl oxygen shown as blue and red spheres, respectively. The gp120 backbone is shown as a cartoon, with the inner domain colored red, the outer domain blue, and the bridging sheet domain cyan. Note that the latter is unfolded in panel b and folded into a β-sheet in panel a.

Peptide triazoles appear to have a unique effect on gp120 conformation. Binding of CD4 to gp120 is accompanied by an unusually large decrease in entropy ($-T\Delta S$ = 44.2 kcal mol^{-1}).[11] This has been suggested to reflect a large conformational change in gp120 by structuring the latter from an ensemble of flexible unstructured states into an activated state [i.e., the CD4-bound state (Figure 1a)].[12] In the activated state, gp120 can be divided into an inner domain, an outer domain, and a minidomain at the inner domain–outer domain interface called the "bridging sheet", where the coreceptor binds (Figure 1a). Folding of the bridging sheet has been suggested to account for half of the structuring in gp120 accompanying formation of the activated state.[13] Peptide triazoles bind with a structuring effect on gp120 ($-T\Delta S$ = 6.3 kcal mol^{-1}) much smaller than that of CD4[11,14] and are proposed to bind to a gp120 conformation different from that of the activated state.[15] It has been suggested that PTs prevent formation of the bridging sheet[14] and effectively "trap" gp120 in a conformation, or an ensemble of conformations, incommensurate with formation of this functionally important domain.[16] The PT-bound state of gp120 thus represents an inactivated "off" state of the glycoprotein.

Currently, there are no crystal structures of a peptide triazole–gp120 complex, hampering efforts to understand the structural mechanism of PT action, optimize the peptide potency, and develop non-natural peptidomimetics through structure-based design. The inherent structural flexibility of gp120,[12,17] combined with incomplete structuring by non-covalently bound PTs,[14] may explain the lack of success to date in obtaining crystals for this complex. One way to overcome this obstacle would be to stabilize the complex into a less flexible state by introducing covalent bonds between the peptide and protein components. A similar approach has been adopted previously to determine the crystal structure of the antigen binding fragment (Fab) of monoclonal antibody b12 with a gp120 core.[17] mAb b12 binds gp120 with a small structuring effect ($-T\Delta S$ = 6.3 kcal mol^{-1}) of the same order of magnitude as that of PTs. Zhou et al. stabilized the b12–gp120 complex for crystallization, by introducing multiple pocket filling and disulfide mutations into gp120.[17] We hypothesized that covalently linking the peptide triazole to gp120 would stabilize the peptide–gp120 complex in a similar fashion.

Recently, we developed a model of the encounter complex between the two molecules.[16] Here, we used that model to guide the design and synthesis of a covalent conjugate of a peptide triazole with gp120. This conjugate exhibits binding properties that argue for occupancy of the PT binding pocket on gp120 by the conjugated peptide. The intramolecularly assembled conjugate holds promise for determining the high-resolution crystal structure of the peptide triazole class of entry inhibitors in complex with gp120. Such assembly of PT and gp120 components also provides experimental support for the molecular dynamics simulation, which in turn can assist in the rational design of peptidomimetic entry inhibitors based on peptide triazoles.

MATERIALS AND METHODS

The following reagents were obtained from the NIH AIDS Reference and Reagents Program, division of AIDS, National Institute of Allergy and Infectious Diseases: anti HIV-1 gp120 monoclonal antibodies 2G12 (H. Katinger) and IgG1 b12 (D. Burton and C. Barbas).

Molecular Dynamics Simulations. Details of the simulations have been explained previously.[16] Briefly, with an all-atom, explicit solvent minimal energy structure of the PT–gp120 core from our previous work as a starting point,[16] a 200 ns equilibration was launched in the *NVT* ensemble with the aim of probing the stability of the complex. The CHARMM22 force field[18] was used with NAMD version 2.7,[19] and all

dx.doi.org/10.1021/bi500136f | *Biochemistry* 2014, 53, 3403–3414

Table 1. Sequences and Functional Properties of Various Peptide Triazole Variants Discussed in This Work[e]

Designation	Sequence	Triazole Derivative	K_D [nM][a]	$IC_{50(ELISA)}$ [nM][b]		$IC_{50(SPR)}$ [nM][c]		Description
				sCD4	mAb 17b	sCD4	mAb 17b	
UM24[14]	Cit[1][d]-N[2]-N[3]-I[4]-X[5][d]-W[6]-S[7]	Ferrocenyl	4.1	-	-	118	138	Representative PT
UM101[16]	Cit[1]-N[2]-N[3]-I[4]-X[5]-W[6]-S[7]	Phenyl	-	230	670	-	-	PT used in modeling
KR21[22]	R[1]-I[2]-N[3]-N[4]-I[5]-X[6]-W[7]-βAla[8]-K(ε-Biotinyl)[9]-G[10]	Ferrocenyl	8	16.5	80	85	110	Biotinylated PT
SR07C	I[1]-N[2]-N[3]-I[4]-X[5]-W[6]-S[7]-S[8]-G[9]-Orn[10][d]-C[11]	Ferrocenyl	23.9	-	-	-	-	PT with C-terminal Cysteine for surface immobilization
PEG-KR21	Linker[19][d]-R[1]-I[2]-N[3]-N[4]-I[5]-X[6]-W[7]-βAla[8]-K(ε-Biotinyl)[9]-G[10]	Ferrocenyl	-	-	-	-	-	Biotinylated PT with a PEG linker
AE21	(Maleimide-Linker-18)[d]R[1]-I[2]-N[3]-N[4]-I[5]-X[6]-W[7]-βAla[8]-K(ε-Biotinyl)[9]	Ferrocenyl	-	-	-	-	-	Biotinylated PT with a PEG linker and a thiol-reactive maleimide

[a] K_D determined using direct binding SPR. [b] IC_{50} determined using a competition ELISA as outlined in Materials and Methods. [c] IC_{50} was determined using competition SPR [d] X = derivatized azidoproline X=(2*S*,4*S*)-4-(4-*Y*-1H-1,2,3-triazol-1-yl) pyrrolidine-2-carboxylic acid where *Y*=phenyl or ferrocenyl; Cit = Citrulline; Orn = Ornithine; Linker19 = 19 Å PEG linker resulting from coupling of N-Fmoc-N″-succinyl-4,7,10-trioxa-1,13-tridecanediamine; Maleimide-Linker-18 = 18 Å PEG linker with a maleimide-reactive end resulting from coupling of (succinimidyl-[(N-maleimidopropionamido)-diethylene glycol] ester) to KR21[e] [e] K_D and IC_{50} values are for WT gp120.

molecular analyses and image renderings were conducted in VMD version 1.9.[20]

Protein Reagents. Soluble CD4 (sCD4) was produced and purified as described previously.[14] Monoclonal antibody 17b was obtained from Strategic BioSolutions. The wild-type (WT) $gp120_{YU-2}$ construct was created by insertion of a V5 (GKPIPNPLLGLDST) coding sequence N-terminal to the C-terminal His_6 tag in a pcDNA3.1 vector carrying the mammalian codon-optimized sequence for a CM5 secretion peptide and $gp120_{YU-2}$ (a gift from N. Madani and J. Sodroski).[21] A Glu to Cys (E275C) mutation was introduced into the YU-2 gp120 backbone using the QuikChange site-directed mutagenesis protocol (Stratagene). The primers were custom-synthesized by Integrated DNA Technologies (IDT). The following primer set was used for E275C: 5′-GATCGT-GATCCGGAGCTGTAACTTCACCAACAACG-3′ (forward) and 5′-CGTTGTTGGTGAAGTTACAGCTCCGGATCACG-ATC-3′ (reverse). Mutagenesis was verified by sequencing (Genewiz Inc.) using the BGHR primer or a custom-made 5′-TCCCCATCCACTACTGCGCCC-3′ primer (IDT). DNA for transient transfection was purified using a QiagenMaxiPrep kit (Qiagene) and transfected into HEK 293F cells according to the manufacturer's protocol (Invitrogen). Five days after transfection had been initiated, cells were harvested and spun down, and the supernatant was filtered through 0.2 μm filters. Purification was performed over a 17b antibody-coupled column prepared using NHS-activated Sepharose (GE Healthcare). gp120 was eluted from the column using 0.1 M glycine buffer (pH 2.4) into 1 M Tris (pH 8.0). The identity of the eluted fractions was confirmed by SDS−PAGE and Western blotting using antibody D7324 (Aalto Bioreagents). After the peak fractions had been pooled, additional purification, including removal of aggregates, was performed with a prepacked Superdex 200 HR gel filtration chromatography column (GE Healthcare). Monomer-containing fractions were identified by SDS−PAGE and Western blotting with mAb D7324, pooled, concentrated, frozen, and stored at −80 °C. $gp120_{WT}$ was biotinylated using EZ-Link-Sulfo-NHS-Biotin, according to the manufacturer's guidelines, and used as a positive control in analyses of the fusion reactions via SDS−PAGE (below).

Peptide Synthesis. Peptide triazoles (Table 1) were produced by manual solid-phase synthesis using Fmoc chemistry on a Rink amide resin at 0.25 mmol scale, purified using reverse-phase HPLC (RP-HPLC), and validated by matrix-assisted laser desorption ionization time-of-flight mass spectrometry (MALDI-TOF MS) as detailed elsewhere.[14] All preparations were initially fractionated on a semiprep Vydac C18 column, and the collected main peaks were then separated on an analytical Luna C18 column. For PEG-KR21 synthesis, a 19-atom PEG linker *N*-Fmoc-*N*″-succinyl-4,7,10-trioxa-1,13-tridecanediamine (Sigma) was introduced N-terminal to the sequence of KR21 (Table 1). The cysteine-containing PT SR07C (Table 1), which was used in SPR studies, was synthesized and purified similarly. For production of the reactive AE21 peptide, lyophilized KR21 was dissolved in methanol and reacted with the heterobifunctional cross-linker $SMPEG_2$ {succinimidyl-[(*N*-maleimidopropionamido)-diethylene glycol] ester} (Pierce) with the latter in 40-fold excess. Typically, the reactions were performed in 200−500 μL volumes at a KR21 concentration of 500 μM. After being incubated for 24 h at room temperature while being vigorously mixed, the reaction mixture was lyophilized, dissolved in triethanolamine (TEA)/acetate buffer (pH 7.0), and immediately injected over a Luna analytical C_{18} RP-HPLC column (Phenomenex) with a gradient of 20 to 70% CH_3CN/(TEA/acetate) over 60 min at a flow rate of 1 mL/min. The integrity of the product and the absence of maleimide hydrolysis were confirmed by MALDI-TOF MS. AE21 was lyophilized and stored at −20 °C as a stock solution in 4 Å molecular sieve-dried DMSO. HPLC chromatograms and MALDI MS spectra for AE21, SR07C, and PEG-KR21 are included in the Supporting Information.

Competition ELISA. Peptide inhibition of binding of sCD4 or 17b to gp120 was assessed via a competition ELISA. $HIV-1_{YU-2}$ gp120 (100 ng) was adsorbed to a 96-well microtiter plate overnight at 4 °C. After being washed three times with PBST [1× PBS with 0.1% Tween 20 (v/v)], the plate was blocked with 3% BSA in 1× PBS for 2 h at room temperature and then washed three times with PBST. All further incubations before detection were conducted in 0.5% BSA in PBS. For sCD4 competition ELISA experiments, 100 μL of sCD4 (0.1 μg mL^{-1}) was added to each well in the presence of increasing concentrations of peptide. After incubation for 1 h, the plate was washed three times followed by addition of 100 μL of biotinylated anti-CD4 antibody OKT4 (eBiosciences) at a 1:5000 dilution. After a 1 h incubation, the plate was washed three times, and 100 μL of streptavidin-conjugated horseradish

dx.doi.org/10.1021/bi500136f | *Biochemistry* 2014, 53, 3403−3414

peroxidase (SA-HRP) was added and incubated for 1 h. The extent of HRP conjugate binding was detected by adding 200 μL of 0.04% *o*-phenylenediamine dihydrochloride (Sigma-Aldrich) in 0.05 M phosphate-citrate buffer for 30 min followed by measuring the optical density (OD) at 450 nm using a microplate reader (Molecular Devices). For 17b competition, a protocol similar to that described above was followed, adding 100 μL of 0.1 μg mL^{-1} antibody to the immobilized gp120 in the presence of increasing concentrations of the peptide. Detection was conducted using an HRP-conjugated rabbit anti-human antibody (Millipore) at a 1:5000 (v/v) dilution followed by OPD development.

Production and Purification of the Peptide−gp120 Covalent Conjugate. Purified gp120 (E275C or WT) was exchanged into reaction buffer [filtered and degassed 0.1 M PBS (pH 6.9) with 10 mM EDTA]. AE21, prepared as a concentrated solution in DMSO, was added to the gp120 solution, and the reaction was continued typically for 4 h. The DMSO content in the reaction mixture was always kept lower than 4% by volume. Typically, reactions were conducted in a volume of 500 μL at gp120 concentrations of 2−10 μM. Initially, a large excess of the reactive peptide ($R_1 = n_{AE21}/n_{gp120} = 40$) was used. However, because we observed that this led to a higher level of nonspecific labeling with WT gp120, we significantly reduced this ratio to 1−2. Maleimide-PEG_2-biotin (hereafter MPB, Pierce) was used as a general-purpose sulfhydryl-directed biotinylation reagent and reacted in parallel with and similar to AE21 with WT or E275C gp120. As a control experiment, AE21 was replaced with the nonreactive KR21 at the same ratios.

The reaction mixture was examined by SDS−PAGE and Western blotting. Blots were probed with α-biotin (mouse monoclonal antibody, Sigma) or α-gp120 (D7324 antibody, Aalto Bioreagents) antibodies. After this analysis, and to remove unreacted peptide and other reagents, the reaction mixture was first buffer exchanged five times into 0.1 M PBS (pH 7.4) using Ultracel 30K filters (Amicon). The resulting mixture (~500 μL) was then dialyzed against a large volume (4 L) of 0.1 M PBS (pH 7.4) using a 10 kDa MWCO Slide-A-Lyzer mini dialysis device (Pierce). CaptAvidin-conjugated agarose beads (Invitrogen) were packed into a small column and used for further purification of the covalent conjugate using fast protein liquid chromatography (FPLC). The sample from the previous step was exchanged into 0.05 M citrate buffer (pH 4.0) via ultrafiltration using Ultracel 30K filters (Amicon). It was then passed over the CaptAvidin column and eluted in 1 mL fractions using 0.05 M carbonate buffer (pH 10.0) into 1 mL of 0.1 M PBS (pH 7.4). The identity of the eluted peaks was confirmed using SDS−PAGE and Western blotting with a mouse α-biotin antibody (Sigma-Aldrich). No residual unreacted AE21 peptide was detected in the final pool of elution peaks.

Surface Plasmon Resonance (SPR) Assays. SPR experiments were performed on a Biacore 3000 optical biosensor (GE Healthcare). All experiments were conducted at 25 °C using standard PBS buffer (pH 7.4) with 0.005% surfactant P-20. A CM5 sensor chip was derivatized by standard 1-ethyl-3-[3-(dimethylamino)propyl]carbodiimide (EDC)/*N*-hydroxysuccinimide (NHS) chemistry, and coupling was accomplished via ligand amine groups. For immobilization of the thiol-containing peptide SR07C, 2-(2-pyridinyldithio)ethaneamine (PDEA) in 0.1 M borate buffer (pH 8.5) was injected over the surface after EDC/NHS activation of the surface dextran matrix. SR07C was coupled to this surface through disulfide exchange. Antibody 2E3 (α-human IL5) or 2B6R (α-human IL5R) was immobilized for use as a control surface. In surface capture experiments, NeutrAvidin−biotin binding protein (NA; Pierce) was immobilized on the surface through standard EDC/NHS chemistry (above), and the reaction mixture was passed over the surface at a rate of 5 μL/min to capture the biotinylated product. To control for the different amounts of product captured on such a surface and E275C-immobilized surfaces, signals were normalized to the maximal signal from injection of 200 nM mAb D7324. For kinetic analyses, typically 200−300 RUs of protein reagents were immobilized on SPR chips, and analytes were passed over the surface at a rate of 50−100 μL/min. Surface regeneration was achieved by a 5 μL injection of a 10 mM HCl solution at a rate of 100 μL/min.

Data analysis was performed using BIAEvaluation version 4.0 (GE Healthcare). Signals from buffer injection and control surface binding were subtracted in all experiments to account for nonspecific binding. For the determination of kinetic parameters, we used a method similar to that used by Morton et al.[22] The signal from the highest concentration of the analyte was used to calculate the off rate (k_d) using a simple 1:1 binding model. For each concentration, the association-phase data were fit to a simple 1:1 bimolecular interaction model using BIAEval. The resulting R_{eq} values were used to fit the corresponding steady state model to calculate equilibrium dissociation constant (K_D) values.

RESULTS

Rational Design of a PT−gp120 Covalent Conjugate. Covalent conjugation of peptide triazole to gp120 was guided by a recently proposed atomistic model of the peptide triazole−gp120 encounter complex.[16] In this simulation, the peptide was bound at the junction of the inner and outer domains, with a gp120 surface epitope overlapping the F43 pocket, and a gp120 conformation in which the bridging sheet did not form. In addition, peptide binding was shown to prevent formation of the bridging sheet and, associated with that, to prevent binding of CD4 and the coreceptor (or coreceptor surrogate antibodies such as mAb 17b). Figure 1b shows the lowest-energy conformation of gp120 in the encounter complex of our model. This can be compared with the CD4-bound form in Figure 1a.

The thiol group on cysteine side chains provides a selective bioconjugation target on proteins.[23] Previous work on disulfide stabilization of the gp120 core has identified multiple double-cysteine mutations that minimally alter the antigenic profile of gp120.[17] In light of our PT−gp120 complex model, the double-cysteine mutation V275C/W96C was especially interesting. Position 275 on gp120 (E275 in the sequence of $gp120_{YU-2}$) is on a sequentially variable loop, on the conformationally fixed outer domain of gp120 and outside the CD4 binding site.[24] Hence, we selected this position for further studies.

The minimal energy conformation from the initial simulation (Figure 1b) was subjected to 200 ns of MD equilibrium to probe its stability and further refine the model. Figure S1 of the Supporting Information shows the rmsd (root-mean-square deviation) trace of heavy atoms for various peptide residues along with the overall peptide rmsd. From this plot, one can see that the N-terminal citrulline is substantially more flexible than the rest of the peptide. This can be better visualized by tracing the coordinates of the N-terminal amine nitrogen of the peptide backbone during the equilibrium as a point of reference

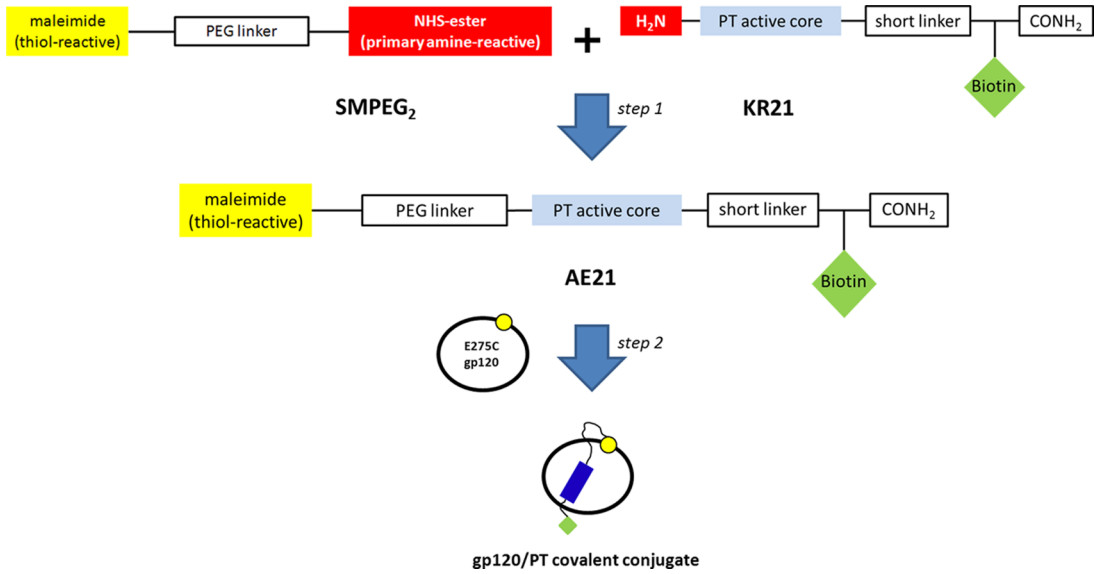

Figure 2. Reaction scheme utilized to produce a gp120−PT covalent conjugate. In step 1, the N-terminal amine of the biotinylated peptide KR21 was reacted with the NHS ester of the heterobifunctional cross-linker $SMPEG_2$ to produce a PEGylated PT bearing a reactive maleimide moiety (AE21). Then this peptide was conjugated to E275C gp120 through the reaction of the maleimide with the thiol group introduced on gp120 via the E275C mutation.

(Figure 1b). The distance from this atom to the side chain (γ-carbon) of E275 was measured during equilibration, and from that, a distance distribution plot was constructed (Figure S2 of the Supporting Information). The mode value for the distribution was found to be ~17.41 Å. This suggests that if the sequence used in the model were to be used to synthesize the reactive peptide, there would need to be a linker of at least ~18 Å connecting the N-terminus of the peptide to the thiol group on E275C. Considering that this is the linear distance between the two measurement coordinates, we expect 17.41 Å to be a minimum for the linker length.

Previous studies have shown that the INNIXW motif is the minimal sequence required for peptide activity.[14] We have recently reported the binding characteristics of a biotinylated PT variant, KR21 (Table 1).[21] The major difference between peptides UM101 [used in simulations (Table 1)] and KR21 is the replacement of a phenyl group on the triazole in the former with a ferrocenyl group in the latter. It has been found that the hydrophobic groups are interchangeable with only modest effects on peptide activity.[7,8] Because the biotin moiety at the C-terminus of KR21 offers a convenient handle for downstream analysis and purification of the covalent conjugate, we chose KR21 as the base for our conjugate production.

Considering the arguments put forward in the previous paragraphs for the required length of an N-terminal linker to connect the peptide to E275C on gp120, a short (~19 Å) PEG [poly(ethylene glycol)] linker was introduced on the N-terminus of the peptide. We hypothesized that the additional N-terminal amino acid on the biotinylated peptide (KR21) compared to the modeled peptide (UM101), combined with the flexibility of a PEG linker, would be sufficient to position a conjugated PT close to its (modeled) binding site on gp120. The KR21 sequence lacks primary amines except on the N-terminus. Hence, we postulated that, using a commercially available heterobifunctional PEG linker with *N*-hydroxysuccinimide (NHS) and maleimide groups on the two ends, we can couple a thiol-reactive maleimide along with the PEG linker to the N-terminus of KR21. A scheme of the approach to design the PT−gp120 covalent conjugate is shown in Figure 2.

Expression and Characterization of a Single-Cysteine, Functional Mutant of HIV-1 gp120. Although previous work has shown that a double-cysteine $gp120_{HxBc2}$ mutant V275C/W96C can be expressed and is functional, no such information was available for similar single-cysteine mutants of gp120. We chose to introduce a cysteine mutation at position 275 [$E275C_{YU-2}$ (shown in Figure 1b with green spheres)] as a connection point on the protein for peptide conjugation. We first tested the binding affinity of the E275C gp120 mutant for various gp120 ligands and compared it to the WT protein. Proteins sCD4 (soluble receptor), mAbs17b (coreceptor surrogate/CD4-induced antibody), and b12 (CD4 binding site antibody) were used as analytes in SPR experiments with chip-immobilized WT or E275C gp120. Kinetic parameters were obtained (Materials and Methods) and the resulting K_D values determined (Table S1 of the Supporting Information). The affinities of sCD4 and 17b for E275C are slightly reduced, though the latter still maintains nanomolar binding affinity for these molecules. Interestingly, the affinity of CD4 binding site mAb b12 for E275C is almost the same as that for WT gp120. These results show that the single-cysteine mutant E275C is functional for binding typical ligands of gp120.

The affinity of the E275C mutant for peptide triazoles was next assessed. A C-terminal cysteine was introduced into the peptide sequence after a short spacer from the active core [SR07C (Table 1)] and used to immobilize the peptide on the SPR chip. Serial dilutions of purified E275C gp120 were passed over the surface, and the resulting sensorgrams were used to extract kinetic parameters of interaction between gp120 (WT and E275C) and PTs (Figure S3 of the Supporting Information). Both proteins bind the peptide with similar affinities, as shown by the value of the equilibrium dissociation constant obtained from the sensorgrams (K_D values of 8.3 nM for WT gp120 and 6.8 nM for E275C). These results confirm that E275C recognizes PTs with an affinity similar to that of

dx.doi.org/10.1021/bi500136f | *Biochemistry* 2014, 53, 3403−3414

WT gp120 and can be a suitable candidate for further modifications.

Synthesis and Characterization of the Biotinylated, PEGylated PT. Maleimides react nearly exclusively with thiols in the pH range of 6.5−7.5.[23] In addition, a diverse array of heterobifunctional cross-linkers with maleimide and *N*-hydroxysuccinimide (NHS) ester functionalities are commercially available from various suppliers. Because the PT variants used in this work lacked side chain primary amines, we introduced the desired PEG linker bearing a maleimide moiety by reacting a heterobifunctional cross-linker of suitable length through its NHS end with the primary amine on the N-terminus of the PT. The resulting approach used to produce a thiol-reactive PT is illustrated in Figure 2.

To probe the likelihood that such a reactive PT would be functionally active, the effect of simultaneously introducing the C-terminal biotin and N-terminal PEG linker during PT−gp120 interactions was first tested using a nonreactive, biotinylated, PEGylated PT. Previously, it was demonstrated that the C-terminal biotin on KR21 has a minimal effect on PT−gp120 interactions (Table 1).[21] A short PEG linker was introduced at the N-terminus of KR21 via solid-phase peptide synthesis, and the activity of the resulting PEG-KR21 PT was tested in a competition assay. Fixed concentrations of sCD4 or mAb 17b were mixed with serial dilutions of PEG-KR21, and the amount of bound sCD4 or mAb 17b was probed using an ELISA (Figure S4 of the Supporting Information). Although these data show a slight decrease in the inhibitory potency of PEG-KR21 relative to that of KR21 for gp120−sCD4 interaction, overall the inhibitory potencies of both peptides for the interaction of gp120 with sCD4 and 17b are fairly similar. Therefore, introduction of the PEG linker at the N-terminus of the PT has only minimal effects on the potency of the peptide toward both WT and E275C gp120 proteins. These results demonstrate the feasibility of obtaining a binding-competent reactive PT.

Formation of a PT−gp120 Covalent Conjugate. The conjugate was produced in two stages (Figure 2). First, a biotinylated, PEGylated, cysteine-reactive PT (AE21) was synthesized through conjugation of a heterobifunctional cross-linker ($SMPEG_2$) to KR21. In the second stage, AE21 was reacted with E275C. After AE21 had been reacted with E275C (Materials and Methods), the reaction mixture was analyzed using SDS−PAGE followed by Western blotting. Because the biotinylated peptide provides a versatile marker (biotin) uniquely identifying the final product, the blot was probed with an α-biotin antibody.

As shown in Figure 3, AE21 successfully biotinylated E275C gp120 (lane 3), as judged by the α-biotin signal at the gp120 molecular weight mark, while KR21 (on which the nonreactive biotinylated PT variant AE21 is based) did not show any signal (lane 2) at the same molecular weight mark. Because the major difference between KR21 and AE21 is the presence of the reactive maleimido group on the latter, and considering that noncovalent intermolecular complexes break up in the chaotropic environment of SDS−PAGE, these results provide evidence that AE21 is reactive for conjugation to E275C gp120.

We next investigated whether binding of the PT to gp120 improves the efficiency of the maleimide−thiol reaction, as expected on the basis of the established tethering approach to fragment-based drug discovery.[25,26] A commercially available, thiol-reactive biotinylation reagent [MPB (Materials and Methods)] was used to label the free cysteine on E275C.

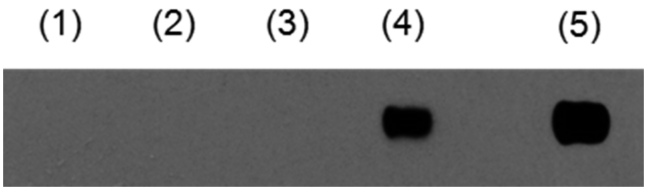

Figure 3. Western blot analysis of the gp120−PT covalent conjugate stained with anti-biotin. (a) Reactivity of AE21 PT probed via SDS−PAGE and Western blotting: lane 1, E275C gp120 only; lane 2, mixture of E275C gp120 and KR21 PT [nonreactive peptide (Table 1)]; lane 3, mixture of E275C gp120 and MPB (commercially available thiol-specific biotinylation reagent); lane 4, mixture of E275C gp120 and AE21 PT; lane 5, biotinylated WT gp120 (positive control). Small-molecule reactants were used in 2-fold excess vs. their protein counterparts.

Biotinylation of E275C gp120 by MPB was found to occur with yields significantly lower than those for AE21 labeling of E275C (Figure 3). This observation suggests that the affinity of AE21 for gp120, which is provided by its PT component, improves the chemical reactivity of the maleimide moiety, likely by localizing it close to the reactive -SH partner on the E275C gp120 surface. These results argue that binding of the PT to E275C gp120 significantly improves the labeling efficiency of the latter by AE21 and promotes formation of the covalent conjugate.

To investigate whether the E275C mutation provides any benefit for the conjugation reaction, AE21 was reacted with WT gp120 and, in parallel, with E275C. The reaction mixtures were analyzed using SDS−PAGE and Western blotting with an α-biotin antibody (Figure 4). To further probe the specificity of

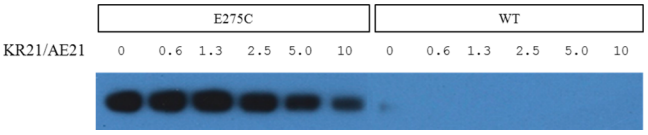

Figure 4. SDS−PAGE followed by α-biotin Western blot analysis of the reaction mixture containing E275C (lanes 1−6) or WT (lanes 7−12) gp120 with a fixed number of AE21-reactive peptide molecules ($R_1 = n_{AE21}/n_{gp120} = 2$, where n denotes moles) in the presence of increasing concentrations of KR21 (the nonreactive peptide).

the AE21−gp120 interaction, the reaction was performed in the presence of increasing concentrations of KR21 (the nonreactive base peptide for AE21). The results showed that binding of AE21 to gp120 significantly improved the labeling of the protein as competition for binding by KR21 led to a reduction in the labeling efficiency (Figure 4, lanes 1−6). Under the same reaction conditions, close to undetectable WT labeling was observed (Figure 4, lanes 7−12). Considering the lack of significant E275C labeling by MPB, and the thousand-fold higher reactivity of maleimide groups toward thiols in the pH range studied here,[23] we conclude that using low excess AE21:E275C ratios would all but abrogate any non-cysteine reactions of AE21. We therefore used an R_1 of 1−2 for all the following reactions.

Overall, the results obtained indicate the successful synthesis of a reactive PT variant, AE21's selective noncovalent binding to gp120, and selective reaction with E275C gp120 to form a covalent conjugate. Together, these argue for selectivity toward the desired site of labeling, corroborating the simulation-based

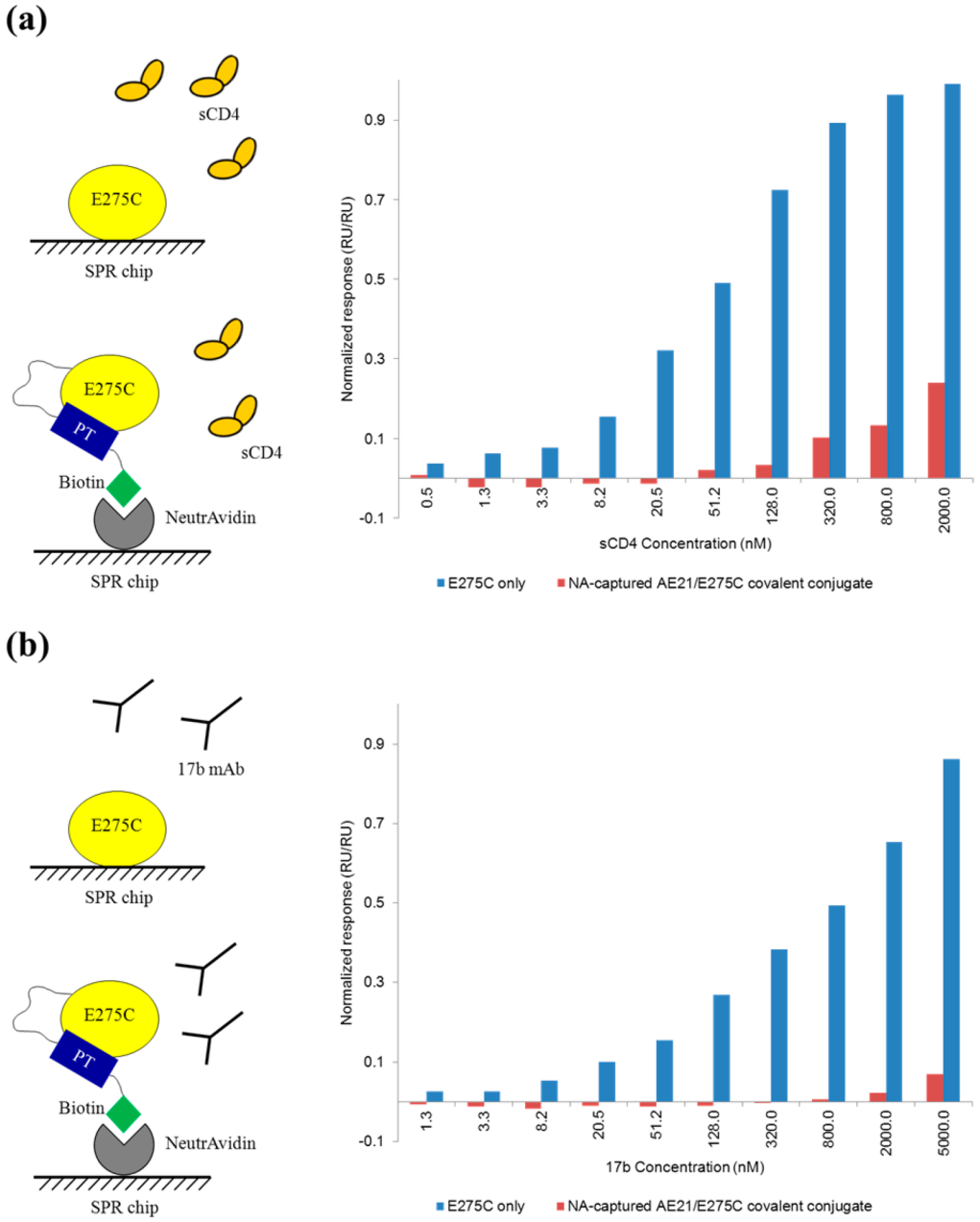

Figure 5. Binding of different concentrations of (a) sCD4 and (b) mAb 17b to E275C and the NeutrAvidin-captured AE21−E275C covalent conjugate, after reference subtraction and normalization to control for the amount of immobilized protein (Materials and Methods). The schematics on the left side of each panel depict the assay configuration. E275C was immobilized on the surface using standard amine coupling (Materials and Methods). The AE21−E275C covalent conjugate was captured from a filtered reaction mixture using surface-immobilized NeutrAvidin via the biotin handle on the peptide. Different concentrations of analytes were passed over the surfaces at a rate of 100 μL/min. Response levels at the end of the association phase (80 s) were used as the representative equilibrium signal at each concentration.

design of the complex and the choice of $gp120_{YU-2}$ E275 for conjugation.

Antibody Binding Characteristics of the gp120−PT Covalent Conjugate. Although the results described above provide evidence that the reactive peptide triazole AE21 labels E275C, the ultimate goal will be a conjugated E275C in which the peptide occupies its "native" binding pocket and the protein adopts the same conformation adopted when the peptide binds noncovalently. One way to probe for these conformational characteristics is by testing the binding of various antibodies to the AE21−E275C conjugate. Binding of the peptide triazole to gp120 did not alter the binding properties of most antibodies that bind linear epitopes on gp120 (e.g., D7324 to the C-terminus of gp120).[27] In contrast, peptide triazoles inhibited binding of most conformational antibodies to gp120. Examples included mAbs F105 and 17b.[15] F105 is an antibody to the CD4 binding site (CD4bs),[28] and 17b is a CD4-induced (CD4i) antibody; i.e., its binding to gp120 is improved in the presence of CD4. It has been suggested that peptide triazoles allosterically inhibit binding of CD4i antibodies, possibly through inhibition of the formation of bridging sheets.[15] From this precedent, the finding that the AE21−E275C covalent conjugate has a reduced binding affinity for CD4bs and CD4i antibodies is expected.

dx.doi.org/10.1021/bi500136f | *Biochemistry* 2014, 53, 3403−3414

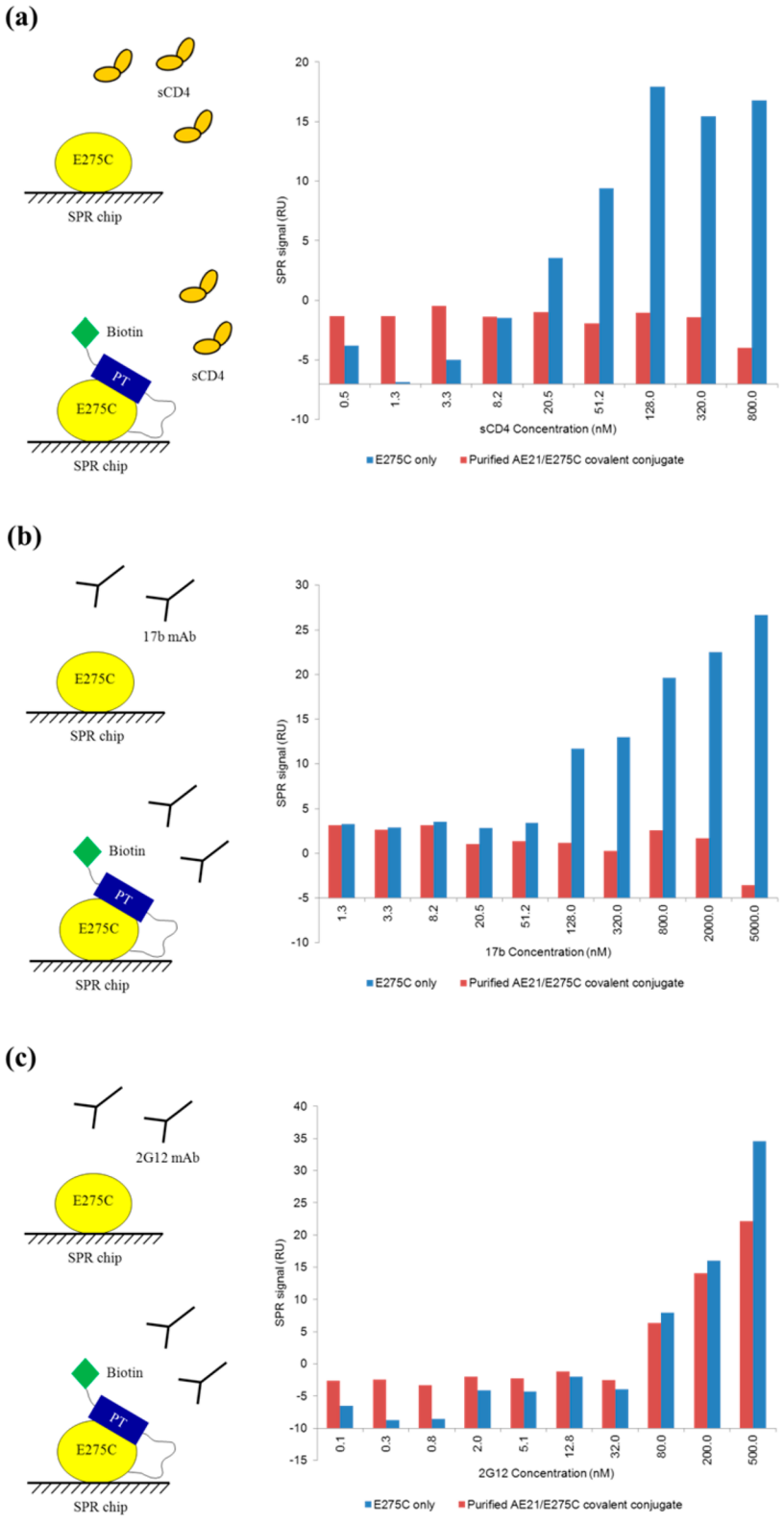

Figure 6. Binding of different concentrations of (a) sCD4, (b) mAb 17b, and (c) mAb 2G12 to E275C and the purified AE21−E275C covalent conjugate. The schematics on the left side of each panel depict the assay configuration. After purification, the covalent conjugate was immobilized using amine coupling, similar to that used for E275C. The response level at the end of the association phase (130 s) was used as the representative equilibrium signal at each concentration. Data are from averages of two independent sensorgrams (n = 2).

Before attempting to purify the covalent conjugate, we tested for CD4 binding with an SPR capture assay. Briefly, NeutrAvidin-biotin binding protein (Materials and Methods) was immobilized on an SPR chip, and the filtered and dialyzed reaction mixture was passed over this surface. Because the only biotinylated components in the reaction mixture are the free AE21 peptide and the AE21−E275C covalent conjugate, and the former was removed via extensive ultrafiltration and dialysis

dx.doi.org/10.1021/bi500136f | *Biochemistry* 2014, 53, 3403−3414

(Materials and Methods), the major component captured on the SPR chip surface was assumed to be the conjugate (any trace amounts of noncovalent complexes are expected to be dissociated during the initial regeneration steps following D7324 injections). sCD4 was then injected onto the surface containing the captured conjugate. We used the SPR signal at the end of the association phase as the representative equilibrium signal for the binding of the sCD4 analyte to the surface. Figure 5a shows the amount of sCD4 bound as a function of sCD4 concentration, for immobilized E275C gp120 compared to the NeutrAvidin-captured AE21−E275C covalent conjugate. To correct for the different immobilization densities of each surface, 200 nM mAb D7324 was first passed over each surface and the sCD4 response was normalized to the maximal response from D7324. The results show that the covalent conjugate has sCD4 affinity significantly reduced compared to that of E275C gp120.

Binding of sCD4 to the covalent conjugate could be inhibited by two possible factors: (1) the presence of the peptide in its binding pocket and consequent inhibition of sCD4−gp120 interaction and/or (2) blocking of sCD4 binding resulting from partial steric hindrance by the presence of the covalently linked peptide. A more stringent test to confirm the binding pose of the peptide on gp120 was sought by assessing 17b interaction. The 17b binding site is far from position 275 of gp120 (Figure 1b). Thus, considering the size of the peptide and the linker length used here, we surmise that binding of 17b to the bridging sheet region of gp120 is unlikely to be inhibited by steric blockade alone with a covalently tethered peptide triazole. The binding affinity of the AE21−E275C covalent conjugate for 17b was tested in an SPR assay similar to that described above for sCD4. The results, in Figure 5b, show that, similar to the case with sCD4, the covalent conjugate has lost its affinity for 17b, and the effect is even more pronounced than for sCD4. The suppression of 17b binding argues that the covalent fusion is assembled structurally with a conformationally altered bridging sheet similar to that postulated to occur in the noncovalent complex.[16] Overall, the SPR experiments show that the level of binding to both sCD4 and CD4i antibodies is significantly reduced in the covalent conjugate.

One drawback to the capture method used above is the uncertainty of the extent to which the NeutrAvidin capture method itself affects the affinity of various gp120 ligands for the AE21−E275C gp120 covalent conjugate. In addition, the control ligand (E275C) is randomly oriented on the surface, while the covalent conjugate is oriented on the surface through binding with NeutrAvidin. Therefore, we pursued further purification of the conjugate using the biotin handle (Materials and Methods).

The CaptAvidin-purified covalent conjugate was immobilized on the SPR chip like the E275C protein, using NHS/EDC coupling, and various concentrations of gp120 ligands were passed over the surfaces. The SPR signals from different sCD4 concentrations are shown in Figure 6a. These data argue that the covalent conjugate does not bind sCD4 even at very high concentrations. Similar results were obtained for 17b, showing a lack of binding to the AE21−E275C covalent conjugate (Figure 6b).

Peptide triazoles have been found[8] to bind to gp120 in the presence of mAb 2G12, a glycan-specific, conformationally sensitive antibody.[29] The 2G12 binding epitope has been suggested to include a noncontiguous patch of glycans on the "silent face" of gp120, i.e., the face opposite the site where mutational data and modeling results suggest that the peptide binds.[16,21] Moreover, because of its noncontiguous binding epitope on gp120, 2G12 is considered a conformational antibody, the binding of which is sensitive to ordered folding of gp120.[15,30] An SPR experiment was conducted using directly conjugated proteins to test for whether 2G12 could bind to the covalent conjugate in the presence of the peptide triazole (Figure 6c). As the equilibrium association signals show, binding of 2G12 to the covalent conjugate is minimally affected by the presence of the peptide. The 2G12 binding provides support that the covalent conjugate can adopt a conformationally ordered state. Together, these results demonstrate successful production of a peptide triazole−E275C covalent conjugate with interaction properties arguing that the peptide component is assembled intramolecularly with gp120.

DISCUSSION

Inspired by past studies of the stabilization of the conformationally flexible gp120 for crystallization,[17] we set out to engineer a stabilized complex of gp120 and peptide triazoles (PTs). PTs bind gp120 with a weak structuring effect, which has impeded efforts toward crystallization of a PT−gp120 complex. One approach to overcoming the problem of incomplete structuring by gp120 ligands has been engineering mutations into the gp120 sequence to increase conformational stability. For example, structure-guided pocket-filling mutations and disulfide stitches were introduced into the core gp120 sequence to stabilize its complex with b12 and b13, two broadly neutralizing antibodies, to determine crystal structures of the antibody complexes.[17,28] Introduction of engineered mutations into the sequence of such a flexible target protein may have the side effect of perturbing its folding properties.[31,32] We hypothesized that covalent conjugation of the peptides onto gp120 could stabilize the protein structure. Such a covalent conjugate might be a useful "bait" for identifying antibodies that can co-bind with PTs by using it for screening of sera. These antibodies can later be used to further stabilize the complex to improve the chances of obtaining a crystallized protein embodying the PT-bound gp120 structure.

In the absence of crystal structures to guide conjugate design, we turned to computational modeling of the peptide−gp120 complex, starting with a recently developed MD-based model.[16] In this model (Figure 1b), the peptide binds at the interface of the inner and outer domains, preventing folding of the bridging sheet and formation of the coreceptor binding site. Analysis of a long MD equilibration of the complex showed that, although flexible, the N-terminus of the peptide remained close to Glu275 of $gp120_{YU-2}$, which was previously mutated to introduce a disulfide between the gp120 inner and outer domains.[17] We hypothesized that introducing a single cysteine at this position should lead to an expressible protein, denoted E275C gp120, which remains functional toward typical gp120 ligands. Further, this would allow us to use various well-established, thiol-selective conjugation chemistries to connect the N-terminus of the peptide to the protein covalently. A second conclusion from analyzing the modeled structure was the need for a linker ∼18−19 Å in length to connect the N-terminus of the peptide to gp120 at position 275.

Surface plasmon resonance analyses showed that E275C gp120 maintained binding affinity for sCD4 and 17b, the two canonical gp120 ligands. Furthermore, like WT gp120, E275C gp120 was recognized by the monoclonal antibody b12. More importantly, analysis of binding of E275C gp120 to SR07C, a

surface-immobilized peptide triazole variant, showed that the peptide was able to bind to E275C with an affinity similar to that of WT gp120. These results demonstrated the feasibility of using E275C gp120 as a minimally altered gp120 variant containing a suitable, selective handle for peptide triazole conjugation. Because there are no other unpaired cysteine SH groups in WT and E275C gp120 proximal to the functionally important and conformationally variable domains of gp120 around the F43 pocket, this mutant may also be used for future efforts in tethering-based strategies[25,26] to screen for potential entry inhibitors that bind to gp120.

With the simulated model of the noncovalent gp120−peptide triazole complex as a guide, a modular approach was used to design a reactive peptide triazole variant, AE21, for covalent conjugation. A PEG linker was introduced onto the N-terminus of the peptide to allow it to reach E275C. Our ELISA results showed that the presence of the linker has no significant effect on the ability of the peptide to inhibit interactions of gp120 with sCD4 and 17b, the two prototypical gp120 ligands. Further, a maleimide moiety was introduced at the N-terminal end of the linker for selective conjugation to the E275C thiol. A peptide variant with a biotin at the C-terminus assisted in product identification and purification using well-established biotin-based approaches. Introduction of the biotin group on peptide triazoles has recently been reported not to considerably affect the affinity of the peptide for gp120.[21]

Reaction of the AE21 affinity label with the recombinantly engineered gp120 Cys variant E275C yielded the desired covalent conjugate. Analysis of the reaction products via SDS−PAGE and Western blotting using an α-biotin antibody showed that the AE21 peptide reacted with E275C and successfully biotinylated E275C. One would expect E275C gp120 to have a reactivity toward AE21 higher than that of nonbinding thiol-reactive molecules. This is similar to the central concept of tethering-based approaches to small-molecule screening,[25,26] wherein the reactivity of fragments toward thiols is increased if they have a finite affinity for the target protein. Consistent with this assumption, a commercially available biotinylation reagent, MPB, had negligible reactivity toward E275C gp120 (Figure 3), which argues for the role of AE21−E275C binding in improving reactivity.

As further evidence of the specific reaction of AE21 with the E275C thiol, we tested the reaction of AE21 with WT gp120. The results (Figure 4) show that no detectable level of WT labeling by AE21 was observed. The PEG-KR21−gp120 ELISA results (Figure S4 of the Supporting Information) provide predictive evidence for binding of the reactive peptide AE21 to gp120. Hence, a lack of WT gp120 labeling by AE21, combined with negligible labeling of E275C gp120 by MPB, provides further evidence of the specific reaction of AE21 with E275C thiol. This latter finding is consistent with the simulation-based approach to the design of the covalent conjugate.

To evaluate binding characteristics of the PT−gp120 covalent conjugate, the purified AE21−E275C reaction product was immobilized on an SPR chip and binding to various gp120 ligands was measured. If the peptide in the covalent complex occupies the same binding pocket it occupies in a noncovalent complex with gp120, the conjugate and the noncovalent complexes should have similar ligand binding signatures. By SPR, we observed a reduced level of binding of sCD4 to the conjugate. Similarly, a reduced level of binding was observed of CD4bs antibodies F105 and b12 (data not shown), consistent with previous work on inhibition of binding of these ligands to gp120 by the parent peptide of PTs, 12p1,[15] and by PTs.[14] A more stringent test of the conformational properties of the covalent complex was mAb 17b binding, because 17b binds to the bridging sheet in gp120[33] and its epitope is far from position 275 of gp120. The SPR results reported here showed that indeed binding of 17b to the AE21−E275C covalent complex is completely suppressed.

Previous work has shown that antibody 2G12 does not compete with binding of the peptide triazole to gp120.[8] Here, SPR analysis revealed that 2G12 bound to the AE21−E275C covalent complex. This reinforces the argument that the AE21−E275C covalent conjugate has binding characteristics similar to those of a noncovalently bound peptide triazole−gp120 complex.

We recognize that introduction of the highly flexible PEG linker onto the N-terminus of the peptide might affect the conformation of this region in the covalent conjugate compared to that of the noncovalent complex. On the other hand, the reduction in the translational entropy of N-terminal atoms as a result of tethering to gp120 may potentially help to stabilize this part of the peptide, which has been found to be tolerant to various substitutions.[14] On the gp120 side, we cannot rule out the possibility of small, local structural changes near the conjugation site. This might be similar to what was observed in the gp120 inner domain of the b12−gp120 complex reported by Zhou et al.[17] In future designs, we can replace the hydrophilic linker with more hydrophobic ones to better stabilize the complex for crystallization efforts.

Trimeric envelope spikes on HIV are the true targets for antibodies and entry inhibitors. Various designs for the generation of soluble trimers with properties that mimic the immunogenic properties of virion-associated spikes have been attempted.[34−36] The significant progress made in the past few years toward the identification of new classes of anti-Env antibodies has provided increasingly more stringent requirements for the antigenic profile of a soluble antigen.[37−39] Previous work has shown that PTs and the 12p1 parent peptide of PTs inhibit binding of various antibodies (F105 and 17b) to soluble trimers as well as monomers.[15] In addition, virus inactivation, gp120 shedding, and membrane poration activities of PTs[40] demonstrate that these inhibitors recognize the trimer on the virus surface. Examination of the binding and antibody-effector properties of PTs to those of recently emerging soluble trimer designs[41] is needed and is currently being initiated. A PT−trimer fusion can be a useful tool for studying the pathway to such inactivated trimer states, through biophysical−thermodynamic methods and ultimately high-resolution crystallography.

In conclusion, with a simulated model of the peptide triazole−gp120 complex as a starting point, a covalent PT−gp120 conjugate was engineered to embody intramolecular interaction properties similar to those of a PT−gp120 noncovalent complex. The covalent PT−gp120 conjugate provides a potentially valuable tool for elucidating the structural properties of the conformationally entrapped inactivated state of HIV-1 Env gp120 induced by peptide triazoles, including by high-resolution crystallographic analysis. If the conformation of the conjugate is sufficiently stabilized, it could be crystallized on its own, or otherwise used to select for antibodies that can co-bind to provide additional stabilization for crystallization. The successful design of the covalent conjugate is consistent with and hence supports the model of the noncovalent PT−gp120 complex determined by molecular dynamics simulation and can

be used as a tool for follow-up simulation. Finally, structures obtained by simulation or crystallographically would be useful for the structure-based design of peptide triazole peptidomimetics.

■ ASSOCIATED CONTENT

Supporting Information

Table S1 and Figures S1−S14. This material is available free of charge via the Internet at http://pubs.acs.org.

■ AUTHOR INFORMATION

Corresponding Authors

*E-mail: Ali.emileh@dartmouth.edu.
*E-mail: cfa22@drexel.edu.
*E-mail: ichaiken@drexelmed.edu.

Present Address

[‖]A.E.: Thayer School of Engineering, Dartmouth College, 14 Engineering Dr., Hanover, NH 03755.

Funding

We acknowledge the National Institutes of Health for support through Grants 5R21AI093248-02 and 5R21AI091513-02 (A.E., C.F.A., and I.M.C.) and 5P01GM056550 (A.E., C.D., A.P.H., A.R.B., R.A., F.T., S.R., H.L., and I.M.C.) and the National Science Foundation (NSF) for computational support through TeraGrid/XSEDE allocation MCB070073N (C.F.A.). Part of the computational work was performed on the DRACO GPU cluster in the Department of Physics at Drexel University (NSF Grant AST-0959884).

Notes

The authors declare no competing financial interest.

■ ABBREVIATIONS

HIV, human immunodeficiency virus; mAb, monoclonal antibody; HPLC, high-performance liquid chromatography; MALDI-TOF MS, matrix-assisted laser desorption ionization time-of-flight mass spectrometry; ELISA, enzyme-linked immunosorbent assay; PBS, phosphate-buffered saline; PBST, phosphate-buffered saline with Tween; BSA, bovine serum albumin; SA, streptavidin; NaCl, sodium chloride; EDTA, ethylenediaminetetraacetic acid; NaOH, sodium hydroxide; HCl, hydrochloric acid; MD, molecular dynamics; Fab, antigen binding fragment; rmsd, root-mean-square distance or deviation; WT, wild-type; IC_{50}, half-maximal inhibitory concentration; EC_{50}, half-maximal effective concentration; PT, peptide triazole; CD4bs, CD4 binding site; CD4i, CD4-induced; SPR, surface plasmon resonance; NHS, *N*-hydroxysuccinimide; SDS-PAGE, sodium dodecyl sulfate−polyacrylamide gel electrophoresis; HPLC, high-performance liquid chromatography; RP-HPLC, reverse-phase HPLC; DMSO, dimethyl sulfoxide; PBST, PBS-Tween; HRP, horseradish peroxidase; OPD, *o*-phenylenediamine dihydrochloride; MWCO, molecular weight cutoff; EDC, 1-ethyl-3-[3-(dimethylamino)propyl]-carbodiimide.

■ REFERENCES

(1) Wyatt, R., and Sodroski, J. (1998) The HIV-1 envelope glycoproteins: Fusogens, antigens, and immunogens. *Science 280*, 1884−1888.

(2) Poignard, P., Saphire, E. O., Parren, P. W., and Burton, D. R. (2001) gp120: Biologic aspects of structural features. *Annu. Rev. Immunol. 19*, 253−274.

(3) Doms, R. W. (2000) Beyond receptor expression: The influence of receptor conformation, density, and affinity in HIV-1 infection. *Virology 276*, 229−237.

(4) Didigu, C. A., and Doms, R. W. (2012) Novel approaches to inhibit HIV entry. *Viruses 4*, 309−324.

(5) Cocklin, S., Gopi, H., Querido, B., Nimmagadda, M., Kuriakose, S., Cicala, C., Ajith, S., Baxter, S., Arthos, J., Martin-Garcia, J., and Chaiken, I. M. (2007) Broad-spectrum anti-human immunodeficiency virus (HIV) potential of a peptide HIV type 1 entry inhibitor. *J. Virol. 81*, 3645−3648.

(6) McFadden, K., Fletcher, P., Rossi, F., Kantharaju, Umashankara, M., Pirrone, V., Rajagopal, S., Gopi, H., Krebs, F. C., Martin-Garcia, J., Shattock, R. J., and Chaiken, I. (2012) Antiviral breadth and combination potential of peptide triazole HIV-1 entry inhibitors. *Antimicrob. Agents Chemother. 56*, 1073−1080.

(7) Gopi, H., Umashankara, M., Pirrone, V., LaLonde, J., Madani, N., Tuzer, F., Baxter, S., Zentner, I., Cocklin, S., Jawanda, N., Miller, S. R., Schon, A., Klein, J. C., Freire, E., Krebs, F. C., Smith, A. B., Sodroski, J., and Chaiken, I. (2008) Structural determinants for affinity enhancement of a dual antagonist peptide entry inhibitor of human immunodeficiency virus type-1. *J. Med. Chem. 51*, 2638−2647.

(8) Gopi, H., Cocklin, S., Pirrone, V., McFadden, K., Tuzer, F., Zentner, I., Ajith, S., Baxter, S., Jawanda, N., Krebs, F. C., and Chaiken, I. M. (2009) Introducing metallocene into a triazole peptide conjugate reduces its off-rate and enhances its affinity and antiviral potency for HIV-1 gp120. *J. Mol. Recognit. 22*, 169−174.

(9) Bastian, A. R., Kantharaju, McFadden, K., Duffy, C., Rajagopal, S., Contarino, M. R., Papazoglou, E., and Chaiken, I. (2011) Cell-free HIV-1 virucidal action by modified peptide triazole inhibitors of Env gp120. *ChemMedChem 6*, 1318 , 1335−1339.

(10) Tuzer, F., Madani, N., Kamanna, K., Zentner, I., LaLonde, J., Holmes, A., Upton, E., Rajagopal, S., McFadden, K., Contarino, M., Sodroski, J., and Chaiken, I. (2013) HIV-1 Env gp120 structural determinants for peptide triazole dual receptor site antagonism. *Proteins 81*, 271−290.

(11) Kwong, P. D., Doyle, M. L., Casper, D. J., Cicala, C., Leavitt, S. A., Majeed, S., Steenbeke, T. D., Venturi, M., Chaiken, I., Fung, M., Katinger, H., Parren, P. W., Robinson, J., Van Ryk, D., Wang, L., Burton, D. R., Freire, E., Wyatt, R., Sodroski, J., Hendrickson, W. A., and Arthos, J. (2002) HIV-1 evades antibody-mediated neutralization through conformational masking of receptor-binding sites. *Nature 420*, 678−682.

(12) Kwon, Y. D., Finzi, A., Wu, X., Dogo-Isonagie, C., Lee, L. K., Moore, L. R., Schmidt, S. D., Stuckey, J., Yang, Y., Zhou, T., Zhu, J., Vicic, D. A., Debnath, A. K., Shapiro, L., Bewley, C. A., Mascola, J. R., Sodroski, J. G., and Kwong, P. D. (2012) Unliganded HIV-1 gp120 core structures assume the CD4-bound conformation with regulation by quaternary interactions and variable loops. *Proc. Natl. Acad. Sci. U.S.A. 109*, 5663−5668.

(13) Myszka, D. G., Sweet, R. W., Hensley, P., Brigham-Burke, M., Kwong, P. D., Hendrickson, W. A., Wyatt, R., Sodroski, J., and Doyle, M. L. (2000) Energetics of the HIV gp120-CD4 binding reaction. *Proc. Natl. Acad. Sci. U.S.A. 97*, 9026−9031.

(14) Umashankara, M., McFadden, K., Zentner, I., Schon, A., Rajagopal, S., Tuzer, F., Kuriakose, S. A., Contarino, M., Lalonde, J., Freire, E., and Chaiken, I. (2010) The active core in a triazole peptide dual-site antagonist of HIV-1 gp120. *ChemMedChem 5*, 1871−1879.

(15) Biorn, A. C., Cocklin, S., Madani, N., Si, Z., Ivanovic, T., Samanen, J., Van Ryk, D. I., Pantophlet, R., Burton, D. R., Freire, E., Sodroski, J., and Chaiken, I. M. (2004) Mode of action for linear peptide inhibitors of HIV-1 gp120 interactions. *Biochemistry 43*, 1928−1938.

(16) Emileh, A., Tuzer, F., Yeh, H., Umashankara, M., Moreira, D. R., Lalonde, J. M., Bewley, C. A., Abrams, C. F., and Chaiken, I. M. (2013) A model of peptide triazole entry inhibitor binding to HIV-1 gp120 and the mechanism of bridging sheet disruption. *Biochemistry 52*, 2245−2261.

(17) Zhou, T., Xu, L., Dey, B., Hessell, A. J., Van Ryk, D., Xiang, S. H., Yang, X., Zhang, M. Y., Zwick, M. B., Arthos, J., Burton, D. R.,

Dimitrov, D. S., Sodroski, J., Wyatt, R., Nabel, G. J., and Kwong, P. D. (2007) Structural definition of a conserved neutralization epitope on HIV-1 gp120. *Nature 445*, 732−737.
(18) MacKerell, A. D., Bashford, D., Bellott, M., Dunbrack, R. L., Evanseck, J. D., Field, M. J., Fischer, S., Gao, J., Guo, H., Ha, S., Joseph-McCarthy, D., Kuchnir, L., Kuczera, K., Lau, F. T. K., Mattos, C., Michnick, S., Ngo, T., Nguyen, D. T., Prodhom, B., Reiher, W. E., Roux, B., Schlenkrich, M., Smith, J. C., Stote, R., Straub, J., Watanabe, M., Wiorkiewicz-Kuczera, J., Yin, D., and Karplus, M. (1998) All-atom empirical potential for molecular modeling and dynamics studies of proteins. *J. Phys. Chem. B 102*, 3586−3616.
(19) Phillips, J. C., Braun, R., Wang, W., Gumbart, J., Tajkhorshid, E., Villa, E., Chipot, C., Skeel, R. D., Kale, L., and Schulten, K. (2005) Scalable molecular dynamics with NAMD. *J. Comput. Chem. 26*, 1781−1802.
(20) Humphrey, W., Dalke, A., and Schulten, K. (1996) VMD: Visual molecular dynamics. *J. Mol. Graphics 14*, 27−38.
(21) Tuzer, F., Madani, N., Kamanna, K., Zentner, I., Lalonde, J., Holmes, A., Upton, E., Rajagopal, S., McFadden, K., Contarino, M., Sodroski, J., and Chaiken, I. (2013) HIV-1 ENV gp120 structural determinants for peptide triazole dual receptor site antagonism. *Proteins 81*, 271−290.
(22) Morton, T. A., Myszka, D. G., and Chaiken, I. M. (1995) Interpreting complex binding kinetics from optical biosensors: A comparison of analysis by linearization, the integrated rate equation, and numerical integration. *Anal. Biochem. 227*, 176−185.
(23) Hermanson, G. T. (1996) *Bioconjugate techniques*, Academic Press, San Diego.
(24) Pancera, M., Majeed, S., Ban, Y. E., Chen, L., Huang, C. C., Kong, L., Kwon, Y. D., Stuckey, J., Zhou, T., Robinson, J. E., Schief, W. R., Sodroski, J., Wyatt, R., and Kwong, P. D. (2010) Structure of HIV-1 gp120 with gp41-interactive region reveals layered envelope architecture and basis of conformational mobility. *Proc. Natl. Acad. Sci. U.S.A. 107*, 1166−1171.
(25) Erlanson, D. A., Braisted, A. C., Raphael, D. R., Randal, M., Stroud, R. M., Gordon, E. M., and Wells, J. A. (2000) Site-directed ligand discovery. *Proc. Natl. Acad. Sci. U.S.A. 97*, 9367−9372.
(26) Erlanson, D. A., Wells, J. A., and Braisted, A. C. (2004) Tethering: Fragment-based drug discovery. *Annu. Rev. Biophys. Biomol. Struct. 33*, 199−223.
(27) Tuzer, F. (2012) Structural basis of HIV-1 GP120 dual receptor site antagonism by peptide triazoles. Ph.D. Thesis, Drexel University, Philadelphia.
(28) Chen, L., Kwon, Y. D., Zhou, T., Wu, X., O'Dell, S., Cavacini, L., Hessell, A. J., Pancera, M., Tang, M., Xu, L., Yang, Z. Y., Zhang, M. Y., Arthos, J., Burton, D. R., Dimitrov, D. S., Nabel, G. J., Posner, M. R., Sodroski, J., Wyatt, R., Mascola, J. R., and Kwong, P. D. (2009) Structural basis of immune evasion at the site of CD4 attachment on HIV-1 gp120. *Science 326*, 1123−1127.
(29) Calarese, D. A., Scanlan, C. N., Zwick, M. B., Deechongkit, S., Mimura, Y., Kunert, R., Zhu, P., Wormald, M. R., Stanfield, R. L., Roux, K. H., Kelly, J. W., Rudd, P. M., Dwek, R. A., Katinger, H., Burton, D. R., and Wilson, I. A. (2003) Antibody domain exchange is an immunological solution to carbohydrate cluster recognition. *Science 300*, 2065−2071.
(30) Trkola, A., Purtscher, M., Muster, T., Ballaun, C., Buchacher, A., Sullivan, N., Srinivasan, K., Sodroski, J., Moore, J. P., and Katinger, H. (1996) Human monoclonal antibody 2G12 defines a distinctive neutralization epitope on the gp120 glycoprotein of human immunodeficiency virus type 1. *J. Virol. 70*, 1100−1108.
(31) Emileh, A., and Abrams, C. F. (2011) A mechanism by which binding of the broadly neutralizing antibody b12 unfolds the inner domain α1 helix in an engineered HIV-1 gp120. *Proteins 79*, 537−546.
(32) Finzi, A., Xiang, S. H., Pacheco, B., Wang, L., Haight, J., Kassa, A., Danek, B., Pancera, M., Kwong, P. D., and Sodroski, J. (2010) Topological layers in the HIV-1 gp120 inner domain regulate gp41 interaction and CD4-triggered conformational transitions. *Mol. Cell 37*, 656−667.
(33) Kwong, P. D., Wyatt, R., Robinson, J., Sweet, R. W., Sodroski, J., and Hendrickson, W. A. (1998) Structure of an HIV gp120 envelope glycoprotein in complex with the CD4 receptor and a neutralizing human antibody. *Nature 393*, 648−659.
(34) Binley, J. M., Sanders, R. W., Clas, B., Schuelke, N., Master, A., Guo, Y., Kajumo, F., Anselma, D. J., Maddon, P. J., Olson, W. C., and Moore, J. P. (2000) A recombinant human immunodeficiency virus type 1 envelope glycoprotein complex stabilized by an intermolecular disulfide bond between the gp120 and gp41 subunits is an antigenic mimic of the trimeric virion-associated structure. *J. Virol. 74*, 627−643.
(35) Nkolola, J. P., Peng, H., Settembre, E. C., Freeman, M., Grandpre, L. E., Devoy, C., Lynch, D. M., La Porte, A., Simmons, N. L., Bradley, R., Montefiori, D. C., Seaman, M. S., Chen, B., and Barouch, D. H. (2010) Breadth of neutralizing antibodies elicited by stable, homogeneous clade A and clade C HIV-1 gp140 envelope trimers in guinea pigs. *J. Virol. 84*, 3270−3279.
(36) Stamatatos, L., Lim, M., and Cheng-Mayer, C. (2000) Generation and structural analysis of soluble oligomeric gp140 envelope proteins derived from neutralization-resistant and neutralization-susceptible primary HIV type 1 isolates. *AIDS Res. Hum. Retroviruses 16*, 981−994.
(37) Zhou, T., Georgiev, I., Wu, X., Yang, Z. Y., Dai, K., Finzi, A., Kwon, Y. D., Scheid, J. F., Shi, W., Xu, L., Yang, Y., Zhu, J., Nussenzweig, M. C., Sodroski, J., Shapiro, L., Nabel, G. J., Mascola, J. R., and Kwong, P. D. (2010) Structural basis for broad and potent neutralization of HIV-1 by antibody VRC01. *Science 329*, 811−817.
(38) Scheid, J. F., Mouquet, H., Feldhahn, N., Seaman, M. S., Velinzon, K., Pietzsch, J., Ott, R. G., Anthony, R. M., Zebroski, H., Hurley, A., Phogat, A., Chakrabarti, B., Li, Y., Connors, M., Pereyra, F., Walker, B. D., Wardemann, H., Ho, D., Wyatt, R. T., Mascola, J. R., Ravetch, J. V., and Nussenzweig, M. C. (2009) Broad diversity of neutralizing antibodies isolated from memory B cells in HIV-infected individuals. *Nature 458*, 636−640.
(39) Walker, L. M., Phogat, S. K., Chan-Hui, P. Y., Wagner, D., Phung, P., Goss, J. L., Wrin, T., Simek, M. D., Fling, S., Mitcham, J. L., Lehrman, J. K., Priddy, F. H., Olsen, O. A., Frey, S. M., Hammond, P. W., Protocol, G. P. I., Kaminsky, S., Zamb, T., Moyle, M., Koff, W. C., Poignard, P., and Burton, D. R. (2009) Broad and potent neutralizing antibodies from an African donor reveal a new HIV-1 vaccine target. *Science 326*, 285−289.
(40) Bastian, A. R., Contarino, M., Bailey, L. D., Aneja, R., Moreira, D. R., Freedman, K., McFadden, K., Duffy, C., Emileh, A., Leslie, G., Jacobson, J. M., Hoxie, J. A., and Chaiken, I. (2013) Interactions of peptide triazole thiols with Env gp120 induce irreversible breakdown and inactivation of HIV-1 virions. *Retrovirology 10*, 153.
(41) Sanders, R. W., Derking, R., Cupo, A., Julien, J. P., Yasmeen, A., de Val, N., Kim, H. J., Blattner, C., de la Pena, A. T., Korzun, J., Golabek, M., de Los Reyes, K., Ketas, T. J., van Gils, M. J., King, C. R., Wilson, I. A., Ward, A. B., Klasse, P. J., and Moore, J. P. (2013) A next-generation cleaved, soluble HIV-1 Env Trimer, BG505 SOSIP.664 gp140, expresses multiple epitopes for broadly neutralizing but not non-neutralizing antibodies. *PLoS Pathog. 9*, e1003618.